Catalytic Reduction of Coomassie Brilliant Blue R-250 by Silver Nanomagnetic Clusters

Madiha Ishaq, Umar Farooq, Muhammad Salman and Muhammad Makhshoof Athar

School of Chemistry, University of Punjab, Lahore 54590, Pakistan

Abstract: The research work represents the synthesis of silver nanoparticles (AgNPs) coated on magnetic iron oxide nanoparticles by chemical reduction and co-precipitation method, respectively. AgNPs were coated on magnetic ironoxide nanoparticles to form $Ag@Fe_3O_4$. AgNPs were characterized by UV-Visible spectroscopy. The magnetic nanoparticles (MNPs) and magnetic nanoclusters (MNC) were characterized by Fourier transform infra red (FTIR) spectroscopy. Bulk density, moisture content and ash content were also determined. These MNCs were used for the reduction of 4-nitrophenol (4-NP) and coomassie Brilliant Blue R-250 (CBBR-250). The parameters such as effect of time, catalyst dosage, concentration of sodium borohydride and concentration of 4-NP and dye were studied. It was found that the catalytic reduction of 4-NP and dye were in 20 minutes by MNCs. Kinetic analysis shows that the pseudo-first-order was found to be linear. It revealed that the use of these MNCs can be considered as a reliable method for the catalytic reduction studies.

Key words: AgNPs, MNCs, catalytic reduction, 4-NP, CBBR-250.

1. Introduction

Silver nanoparticles (AgNPs) are attractive catalysts due to their exceptional electrical, optical and surface properties. AgNPs have intensive importance in various reactions due to their significant catalytic activity, chemical stability and eco-friendly nature. On the other hand, they are difficult to recycle and reuse because they are carried in solution [1]. So, many supports can be used as polymer, hydrogels, porous monoliths, metal oxides, silicates, colloids and porous carbon for loading AgNPs for their repetitive uses.

The separation and centrifugation of AgNPs depends on their particle size and density, which is probable ultra-centrifugation speed (> 15,000 rpm) [2]. Various methods such as chromatography, cloud point extraction, centrifugation and filtration have been developed for removal, separation and concentrating the nanoparticles from aqueous media. These methods have many problems such as; expensive instrumentation, time consuming, low sample recoveries and background changes (deflection in absorbance). There is a need for the development of a simplified compact process that provides adequate separation with minimum loss. Magnetic nanoparticles (MNPs) can offer a valuable separation method for AgNPs separation, prior to their determination by spectroscopic technique. These magnetic particles can be readily attracted by an external magnet but do not remain permanently magnetized after the field is removed. Magnetic separation offers simplicity and overcomes many of the problems associated with conventional separation techniques. Therefore, magnetic particles coated with AgNPs could be readily separated from the bulk solution. Magnetic particles are advantageous as a capture media for AgNPs, so these are easily separated from suspension by using magnet [3].

These MNPs are attracting significant attention due to their high magnetic properties, large surface area, high thermal stability, high mechanical strength, and less toxicity. In addition, MNPs can be quickly synthesized, have high separation efficiency, are cost effective. MNPs have been utilized for the purification of wastewater by removing dyes and heavy metals,

Corresponding author: Madiha Ishaq, MPhil, School of Chemistry, University of the Punjab Lahore-54590, Pakistan.

alkalinity, and hardness, as well as natural organic compounds and salt. This is due to their simple synthesis, easy optimization of their size and morphology, and the fast magnetic separation under an external magnetic field [4].

A range of methods have been reported for the synthesis of stable, shape controlled and biocompatible iron oxide MNPs. Mwilu et al. [5-8] synthesized the high quality iron oxide NPs by co-precipitaion, thermal decomposition, hydrothermal synthesis and sonochemical methods. Among these, co-precipitation was found to be a simple and conventional method for synthesize of iron oxide NPs, in which, Fe^{2+}/Fe^{3+} salts are used in alkaline medium at high temperature in inert medium. Factors affecting size, shape and composition of MNPs were found to be the type of salt, Fe^{2+}/Fe^{3+} ratio, temperature, reaction time, pH and ionic strength of medium.

$$2Fe^{3+} + Fe^{2+} + 8OH^- \rightarrow Fe_3O_4 + 4H_2O \qquad (1)$$
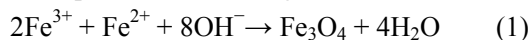
Magnetic particles are widely used in magnetic drug targeting, magnetic resonance imaging for clinical diagnostic, recording material, and biomedical applications because it is non-toxic and easily prepared. Magnetic particles are used as nanosorbents for removal of pollutants (organic or inorganic), heavy metals and many other complex compounds, as photocatalyst in the removal of organic contaminants [9].

AgNPs have been reported for their use as catalyst in conversion of 4-nitrophenol (4-NP) to 4-aminophenol (4-AP) compound, ethylene to ethylene oxide and CO to CO_2 [10, 11]. The AgNPs were used as a catalyst in the degradation of organic dyes such as Alizarin Red S and Remazol Brilliant Blue R [12], methylene violet, eosin methylene blue, safaranin and methylene orange [13, 14]. AgNPs were used in the reduction of methylene blue dye in the presence of $NaBH_4$ [15]. Silver core shells are used as catalyst for methylene blue removal [16]. Modified silver nanoparticles are used for the degradation of organic dyes [17].

Coomassie Brilliant Blue R-250 (CBBR-250) is a triarylmethane dye with chemical formula $C_{37}H_{34}N_2Na_2O_9S_3$. It is a synthetic dye produced by the condensation of 2-formylbenzenesulfonic acid and the appropriate aniline followed by oxidation. The dyes are used in textile, dyeing, paper printing and color photography. These are used in textile industries due to their better fastness to the applied fabric, high photolytic stability, high solubility and resistance to microbial attack. It is frequently used as a starting material in the production of polymeric dyes [18]. It represents an important class of toxic, carcinogenic and mutagenic dye. It is also a recalcitrant organopollutant. It is the cause of skin irritation, allergic dermatitis, dysfunction of kidney, liver, brain, reproductive and central nervous system. The release of dyes causes the inhibitory effect on the process of photosynthesis. It also affects the aquatic life as well as human beings. The catalytic degradation using recyclable nanocatalyst is advantageous to many other methods due to ease of operation, cost-effectiveness, greater efficiency, fast process and no production of secondary sludge. The coating of AgNPs on magnetic nanoparticles eliminates the probability of water pollution by freely available AgNPs.

In the present studies, the silver magnetic nanoclusters (MNCs) are used for the catalytic reduction of CBBR-250 dye. The MNCs are used for the reduction of 4-NP as experimental model reaction. Various factors such as effect of time, catalyst dose, and concentration of reducing agent, dye concentration and pH have been studied. The efficiency of MNC has also been compared with other Ag catalysts in terms of time and amount of catalyst.

2. Experimental

2.1 Preparation of AgNPs

AgNPs were prepared by chemical reduction process as reported, with slight modification [19]. A known volume of $NaBH_4$ [0.02 M, 30 mL] (freshly prepared, before the experiment) was added in beaker

(having magnetic stir). Then, the beaker was positioned in ice bath on a stirring plate. Ice bath was used to slow down the reaction, for efficient particle shape and size. The liquid was stirred and cooled for about 20 minutes. Now, 3% polyvinylpyrolidone (PVP) solution (33 mL) was added in it. PVP is used for prevention of aggregation and also for stabilization of nanoparticles. Silver nitrate (0.01 M) was added in the $NaBH_4$ solution (1 drop per second), stirring until 3 mL of silver nitrate was added. Now, the brown color of the solution indicated the synthesis of silver nanoparticles. A small volume of this solution was taken and diluted it and scanned a UV-vis. The sharp peak at 400 nm is indicated the synthesis of AgNPs. The reduction of silver nitrate can be written as [20]:

$$AgNO_{3(aq)} + NaBH_{4(aq)} \rightarrow Ag_{(s)} +$$
$$\tfrac{1}{2}H_{2(g)} + \tfrac{1}{2}B_2H_{6(g)} + NaNO_{3(aq)} \qquad (2)$$
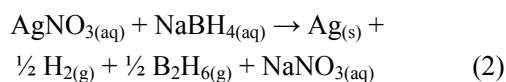
2.2 Synthesis of Magnetic Particles

Magnetic particles were prepared as reported in literature with little changes [21]. Briefly, ferrous sulphate [$FeSO_4 \cdot 7H_2O$ (6.95 g)] and ferric sulphate [$Fe_2(SO_4)_3$ (10 g)] were dissolved in 250 mL deionized water in a 500 mL beaker. Ammonium hydroxide [NH_4OH (25%)] was added slowly for adjusting the pH to 10 of the solution. The reaction mixture was kept at 60 °C. The formed magnetic particles were magnetically separated, washed with deionized water for neutralizing and then dried in oven at 60 °C for 2 h.

2.3 Preparation of Magnetic Nanoclusters (MNC)

AgNPs were doped on magnetic particles by exposing 0.001 mg/mL AgNPs solution to 1 mg/mL magnetic particles for adsorption of AgNPs. Briefly, magnetic particle was added to AgNPs suspension, the mixture was shaken for 30 min at 100 rpm for dispersion of particles. Then it was incubated for 15 min ($T = 60$ °C) to facilitate adsorption of AgNPs. The AgNPs were adsorbed on the iron oxide nanoparticles. These doped particles were magnetically separated

from the suspension [21]. Now, these Ag coated magnetic particles are known as MNCs.

2.4 Characterization

MNCs were oven dried at 60 °C, recorded Fourier transform infrared (FTIR) spectra on FTIR spectrometer (Carry 630, Agilent Technology, USA) with attenuated total reflectance (ATR) mode, in infrared range of 4,000-400 cm^{-1} to evaluate their structural hierarchies. For this purpose, a small amount material was placed on the crystal area and force was applied to the sample by accurately positioning the pressure arm on top of the ZnSe crystal. Different peaks were appeared on the FTIR spectrum.

The amount of Ag on MNC was determined by the AAS (Atomic absorption spectroscopy) by digestion method.

2.5 Catalytic Reduction of 4-NP

To study the catalytic behaviour/effiecinecy of MNC, model reduction reaction of 4-nitrophenol was used. A fixed amount of catalyst was added in a quartz cuvette cotnaining 4NP (50ppm,1mL) and NaBH4 solution. The reaction was monitored by measuring the absorbance in 200-500 nm region. The decrease in absorbance is ploted against reaction time

2.6 Catalytic Behaviour for CBBR-250

The efficiency of MNC as catalyst for the reduction of CBBR-250 was studied by optimizing various factors (time, pH, conc. CBBR-250, $NaBH_4$, dose of catalyst).

For time factor, 1 mL of $NaBH_4$ (10 mM), 1 mL of CBBR-250 (0.04 mM) and 50 mg of catalyst were taken in a UV cuvette and made volume up to 3 mL with distilled water. In other cuvette, the blank (sodium borohydride and MNCs) was taken. UV-visible scan was taken in 200-800 nm wavelength range after each minute until colour disappears. The same procedure was repeated in the absence of catalyst.

The reduction of brilliant blue dye was studied at different amounts of catalyst (25, 50, 75 and 100 mg), and constant concentration of $NaBH_4$ (10 mM) and 1 mL of CBBR-250 (0.04 mM). The reaction was carried out in cuvette; 1 mL of CBBR-250, 1 mL of $NaBH_4$ and $Ag@Fe_3O_4$ were added and volume was made up to 3 mL with distilled water. The absorbance was scanned after regular interval of time.

The effect of concentration of $NaBH_4$ was also studied while keeping concentration of CBBR-250 (0.04 mM) and MNCs (50 mg) constant. The concentration of $NaBH_4$ used is 10, 20, 50, 75 and 100 mM. The reaction was carried out in cuvette, 1 mL of CBBR-250, 1 mL of $NaBH_4$ and $Ag@Fe_3O_4$ were added and volume was made up to 3 mL with distilled water. The absorbance was scanned after regular interval of time.

The concentration of CBBR-250 was varied from 0.01, 0.02, 0.04, 0.05 to 0.06 mM. The amount of catalyst (50 mg) and sodium borohydride (10 mM) were kept constant. The volume in cuvette was made up to 3 mL (1 mL dye solution, 1 mL of sodium borohydride) with distilled water. The absorbance was scanned after regular interval of time.

To study the effect of pH, the pH of solution various between 2, 6, 8 and 10. The constant concentraions of 1 mL of CBBR-250 (0.02 mM), 1 mL of sodium borohydride (10 mM) and catalyst were taken in test tubes. Firstly the pH is adjusted, then add it in cuvette, which made volume up to 3 mL (1 mL dye solution, 1 mL of sodium borohydride) with distilled water. The absorbance was scanned after regular interval of time.

The kinetics of the reduction of CBBR-250 was also studied using Eq. (3). The value of K_{app} was determined and compared with that reported in literature.

$$\ln(A_t/A_o) = \ln(C_t/C_o) = -Kapp \times t \qquad (3)$$

where A_t and A_o are the values of absorbance at any time and at 0 min respectively. C_t and C_o are the values of concentration corresponding to absorbance A_t and A_o respectively. K_{app} is the apparent rate constant.

3. Results and Discussions

3.1 Characterization

3.1.1 UV-VISIBLE Spectrum

The UV-visible spectrum represents the result of surface plasmon resonance (SPR). The SPR of AgNPs is influenced by the size, shape, interparticle interactions, free electron density and surrounding medium, which indicates that it is an efficient tool for monitoring the electron ejection and aggregation of NPs. It is the strong interaction of metal nanoparticles with light resulting in the collective oscillation of the conduction electrons on the metal surface. The SPR results in unusually strong scattering and absorption properties. The formation of AgNPs is indicated from the change in the color from yellow to dark brown. The SPR peak shifted to higher wavelength 423, 425, 423 and 419 nm with increasing silver salt concentration. At higher $AgNO_3$ content, the synthesized AgNPs combined with each other to create a group of aggregations. Thus, the particle size of AgNPs increases with increasing silver salt content. The presence of sharp peak at 300-400 nm is the indication of AgNPs as shown in Fig. 1 [15]. Any information about the size distribution of AgNPs (related with color) can be obtained by analyzing the spectra. The absorption maximum increases as more nanoparticles are formed.

The concentration of silver nanoparticles exhibited an absorption extinction peak at 400 nm with a varying intensity and bandwidth resulting from the varying size and size distribution of the particles. Furthermore, the increasing integrated peak area of the band indicates decrease in interparticle spacing, which is evidence of aggregation [22].

3.1.2 FTIR Spectrum

The FTIR spectral analyses of pure Fe_3O_4 and Ag-Fe_3O_4 nanoparticles are shown in Fig. 2. The spectrum of Fe_3O_4 indicated the absorption band at
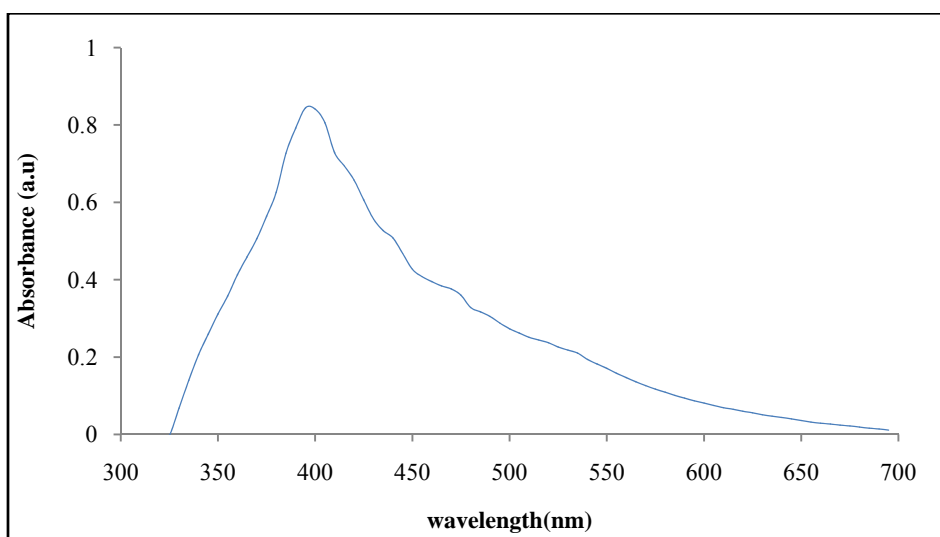
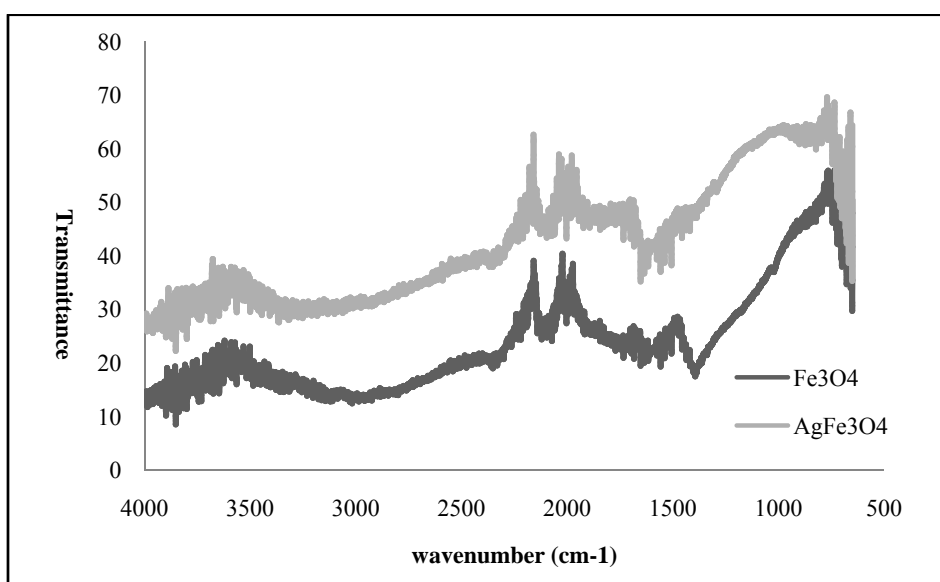**Fig. 1 UV-visible spectrum of silver nanoparticle dispersed in water.**

Fig. 2 The FTIR spectra of MNCs.

2,122, 1,656 and 1,408 cm^{-1}. While, the FTIR spectrum of Ag@Fe$_3$O$_4$ shows that there is slight difference in peaks at 2,111, 1,656 and 1,459 cm^{-1}. FTIR spectra in Fig. 2 show that very strong band at 667 nm^{-1} is assigned to the Fe-O bond, which confirms the presence of magnetic nanoparticles [23]. The stretching vibrations of Fe-O were weakened and red-shifted. The broad absorption band near 3,300 cm^{-1} was due to O-H stretching [24]. The peak at 1,645 cm^{-1} should be due to C = O stretching vibrations of the PVP [25]. The peaks at

1,656 cm^{-1}, 1,395 cm^{-1} are indicated the carbonyl groups (due to water associated with solid particles) [8]. These FTIR spectra provided the useful information that the Fe$_3$O$_4$ was successfully bound to the AgNPs.

3.1.3 Physical Parameters of Magnetic Nanoclusters

The physical parameters such as bulk density, moisture content and ash content were found to be 1.26 g/cm^3, 4.65% and 83% respectively. It was determined by AAS that 100 mg of MNC determined only 0.1 mg of AgNPs.

3.2 Catalytic Activity of MNC for 4-Nitrophenol

The catalytic activity of the silver magnetic nanoclusters was investigated by using them as catalysts for the reduction of 4-NP into 4-AP by using NaBH$_4$. The reduction 4-NP was used as a model experiment to study the catalytic activity. The reduction of 4-NP into 4-AP is also important from an environmental point of view. MNC used as catalyst can be recycled from the reaction mixture easily. The conc. of MNC in the reaction mixture was kept very low as compared to that of 4-NP to avoid any disturbance in absorption spectra. As shown in Fig. 3, the absorbance at 400 nm decreases gradually with the passage of time while that at 300 nm increases with time, which indicates the rapid reduction of 4-NP into 4-AP.

The catalytic reduction of 4-NP is obtained by measuring the absorbance of 4-NP at 400 nm with a time interval of 2 min in the presence of catalyst (50 mg), NaBH$_4$ (10 mM, 1 mL) and 4-NP (50 ppm, 1 mL). With the passage of time, the absorbance at 400 nm decreases and the absorbance at 300 nm increases [26]. The decrease in absorption at 400 nm indicates the reduction of 4-NP and increase in absorption at 300 nm indicates the formation of 4-aminophenol. It is also indicated by the color change from yellow to colourless. In the absence of the catalyst, there is no change in the value of absorbance at 400 nm which indicates that the reduction reaction of 4-NP does not occur without catalyst (Ag@Fe$_3$O$_4$). By using catalyst (Ag@Fe$_3$O$_4$), 4-NP is completely reduced into 4-AP within 20 min.

In the present work, only 0.05 mg AgNPs reduced 4-NP into 4-AP from 50 mg of Ag@Fe$_3$O$_4$. The less amount of Ag@Fe$_3$O$_4$ (0.05 mg) is used in 20 min for the reduction of 4-NP into 4-AP in less time (20 min) as compared to literature. The 4-nitrophenol was reduced in 75 min by silver nanoparticle [27]. The CuO@Ag^0 (0.05 mg) reduced PNP in 22 min [28]. The Fe$_3$O$_4$@PPy-MAA/Ag catalyst (2.5 mg) reduced 4 NP in 45 min. The 4-NP also reduced in 8 min by using silver nanoparticles [29].
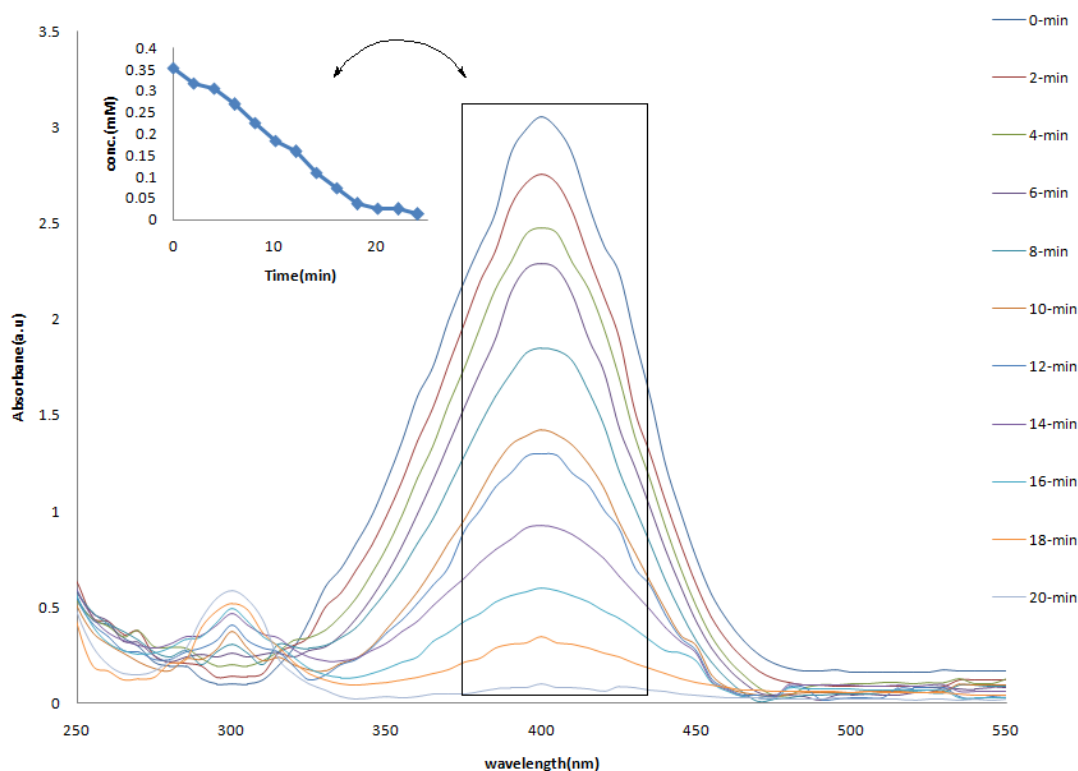

Fig. 3   Time dependent UV-Visible spectra for catalytic reduction of 4-NP into 4-AP (50 mg MNCs, 1 mL of 10 mM NaBH$_4$ and 1 mL of 0.36 mM 4-NP).

3.3 Effect of Different Parameters on the Reduction of CBBR-250

3.3.1 Effect of Time for Reduction of CBBR-250

The CBBR-250 is an aromatic dye and its UV-Visible band (λ_{max}) appears at 550 nm. The progress of the reaction was monitored by measuring the variation in absorbance with time. The UV-Visible spectra (Fig. 5) give maximum absorbance value at this 550 nm. With the passage of time this value of absorbance decreases and after 20 min the absorbance value becomes constant. The relative conc. is plotted as a function of time to evaluate the reduction rate. As shown in Fig. 4, the dye color disappears, which shows that the dye reduction time is very small as compared to early reported literature. Alizarin Red S is degradated in 60 min and Ramazol BBR-250 is degradated in 90 min by AgNPs [12]. Methyl orange is degradated in 17-21 min by AgNPs. While the degradation of eosin methylene blue by biosynthesized silver nanoparticle is in 30 min [13]. The degradation of methyl orange dye (0.95%) was recorded in 30 min by EugeAgNPs (3 mg) [30]. The Fe_3O_4@PDA-Ag microspheres (5 mg) degradated MB (10 mL) in 10 min [16]. The Amp-AgNP (10 mg) reduced methyl green dye in 4 min. The Fe_3O_4@His@Ag MRC (1 mg) decolorized methyl orange (10 mM) in 8 min [31]. The comparative studies of different nanomaterials is also mentioned as shown in Table 1.

3.3.2 Effect of Catalyst

The effect of catalyst dose on the reduction of the dye was investigated as well. The amount of catalyst is the main parameter for the reduction studies. By increasing the conc. of catalyst (50 to 125 mg) while conc. of $NaBH_4$ (10 mM) and CBBR-250 (0.04 mM) was kept constant, an increase in the reduction efficiency of dye was observed. The catalytic reduction decreases slowly as the catalyst dosage increased as shown in Fig. 6. This is due to increase in the No. of active sites on the catalyst by increasing its amount.

When the catalyst amount was more than 50 mg the catalytic efficiency kept constant. The advantage of higher conc. is not limited, and there is the disadvantage of using higher amount of catalyst. Therefore the catalyst amount of 50mg was taken for investigating the other reaction parameters. This is consistent with other reports of catalytic reduction of dyes. The Au/CeO_2-TiO_2 catalyst (433 mg) amount is taken for MB catalytic degradation studies [32]. The catalyst Au@polypyrrol/Fe_3O_4 hollow capsule (2 mg) was reduced methylene blue [33].

Fig. 4   A = original CBBR-250 solution, B = CBBR-250 and MNCs, M = magnet and C = CBBR-250, MNCs and sodium borohydride.
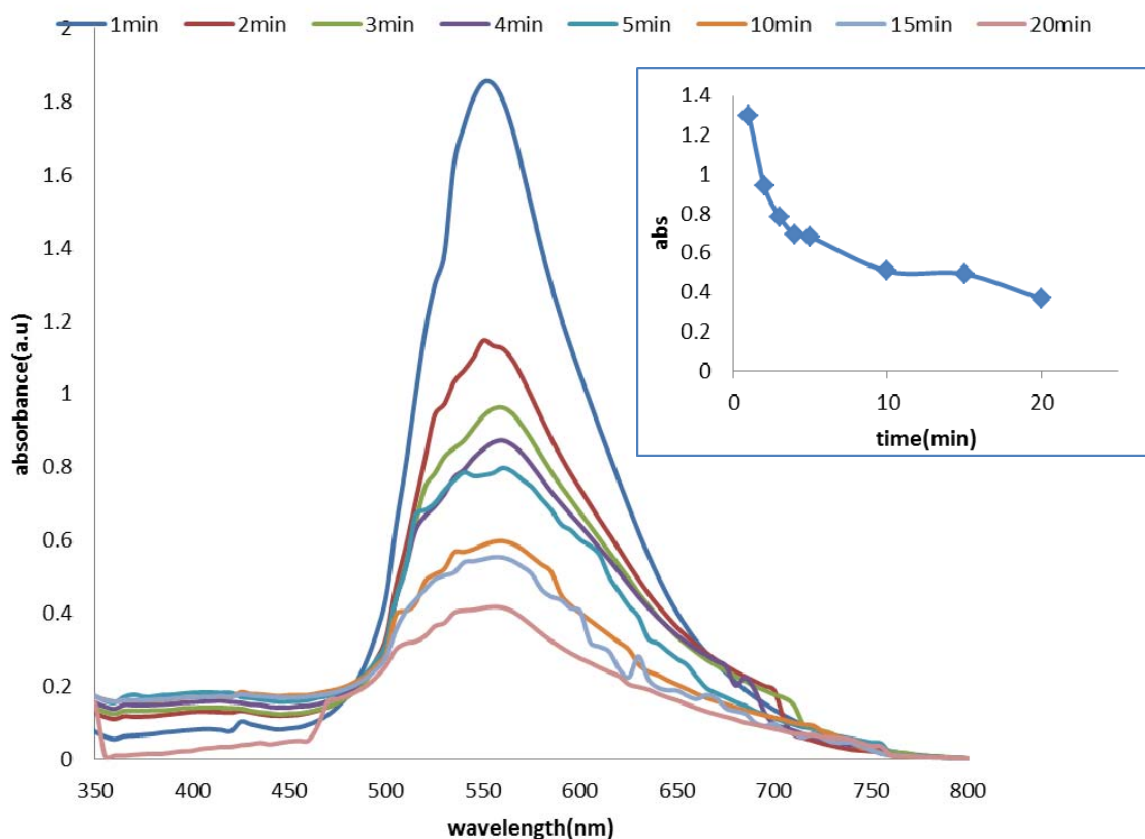
Fig. 5 **Time dependent UV-Visible spectra for catalytic reduction of CBBR-250 dye in the presence of 50 mg MNCs, 1 mL of 10 mM NaBH$_4$ and 1 mL of 0.06 mM CBBR-250.**
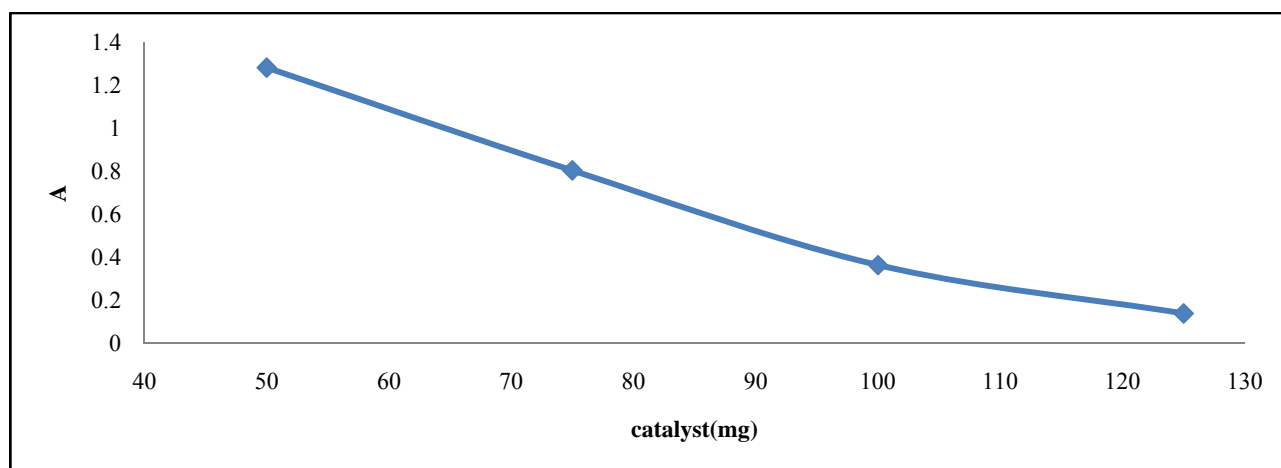

Fig. 6 **UV-Visible spectra for catalytic reduction of CBBR-250 in the presence of (50, 75, 100 and 125 mg) MNCs, 10 mM NaBH$_4$ and 0.04 mM CBBR-250.**

3.3.3 Effect of CBBR-250 Concentration

The effect of conc. of dye is investigated by varying the dye conc. and keeping other parameters constant. By increasing the conc. of CBBR-250 the absorbance value increases slightly as shown in Fig. 7. In other words, the higher concentration of CBBR 250 somehow deactivates the catalytic sides, and catalytic efficiency kept constant. Here, the advantage of higher conc. is limited and there are significant disadvantages of using higher conc. of dye.
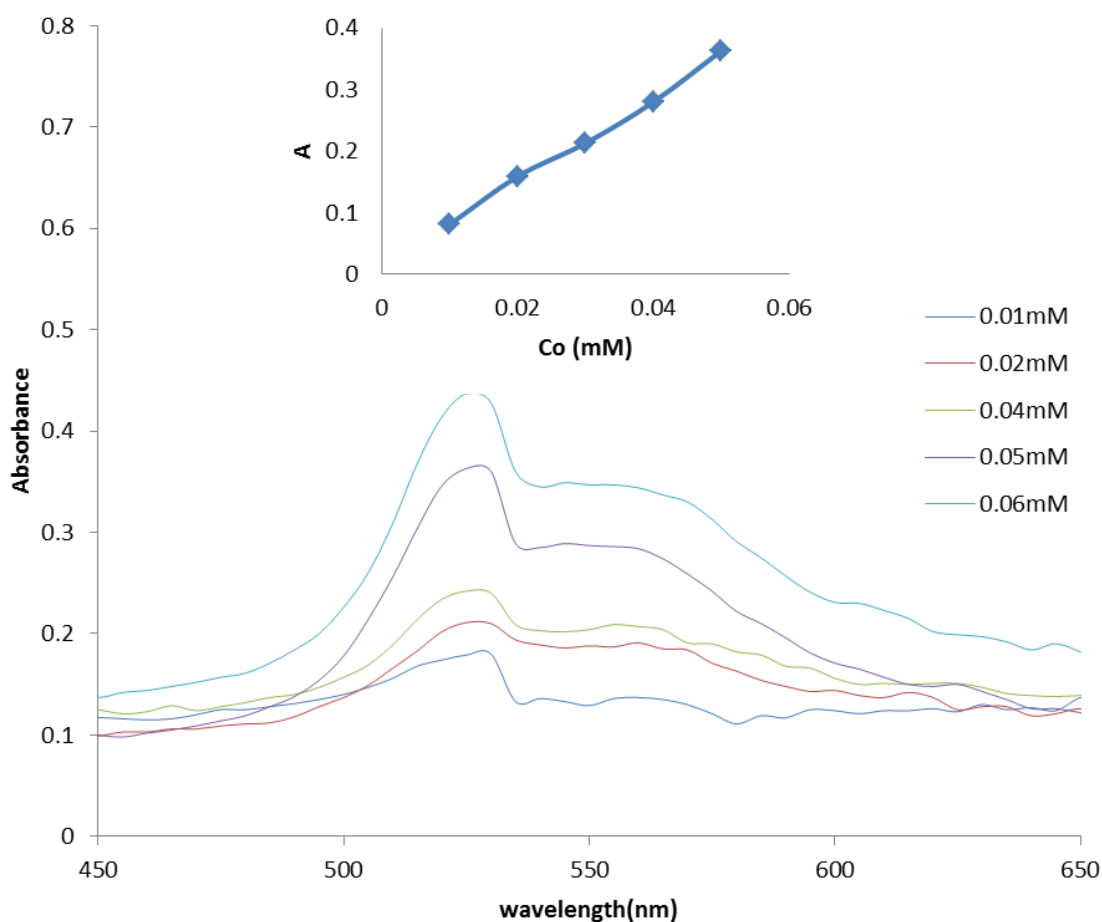
Fig. 7 UV-Vis spectra for catalytic reduction of CBBR-250 in the presence of 50 mg MNCs, 1 mL of 10 mM NaBH₄ and 1 mL of 0.01, 0.02, 0.04, 0.05 and 0.06 mM CBBR-250.

3.3.4 Effect of NaBH₄ Concentration

The effect of change in the concentration of NaBH₄ (10, 50, 75 and 100 mM) on the reduction of CBBR-250 was examined by using Ag@Fe₃O₄ catalyst, keeping rest of the conditions identical (dye 0.04 mM, MNCs 50 mg). These experiments evidently reveal that NaBH₄ variation from 10 to 100 mM, virtually changes the absorbance decrease (as in Fig. 8). In other words, 10 mM NaBH₄ is the optimum amount for the reduction reaction. The mole ratio for NaBH₄ with dye is 1:1.

When the conc. of NaBH₄ was more than 20 mM the catalytic efficiency kept unchanged. The advantages of higher conc. are limited and there are significant disadvantages of using higher conc. of NaBH₄, because of its overabundance. So, most would

be wasted because of limited substrate available. Therefore, increasing the conc. of NaBH₄ beyond its optimal level would not actually promote the efficiency of the process.

3.3.5 Effect of pH

In order to study the pH sensitivity of the prepared catalyst, the effect of pH on the dye (BBR-250) solution is illustrated in Fig. 8. During the degradation studies of CBBR-250, various interactions occurred between NMCs and CBBR-250 dyes such as ion exchange, chemical bonding, physical adsorption and dye-dye interactions etc. [34]. It also determines the surface charge properties of the catalyst and size of aggregates it forms.

The effect of pH on the degradation of dye was studied at 2, 6, 8 and 10. At these pH values the
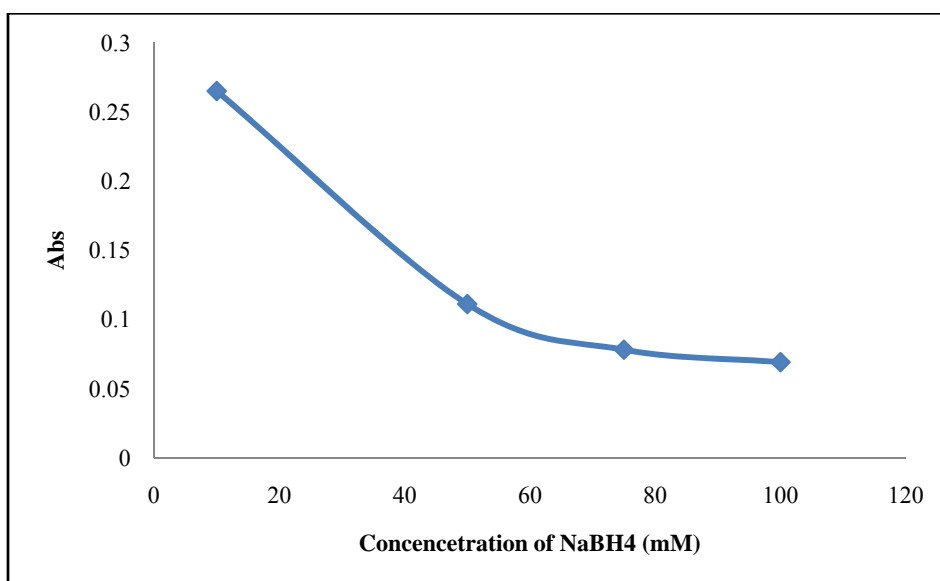
Fig. 8   UV-Visible spectra for catalytic reduction of CBBR-250 in the presence of 50 mg MNCs , 10 mM, 50 mM, 75 mM and 100 mM NaBH₄ and 0.04 mM CBBR-250.

degradation rate declined with different manner as shown in Fig. 9. At lower pH, part of functional groups accommodated on the surface of nanoparticles gets protonated and acquires positive charge. Thus, the electrostatic interaction occurred between nanoparticles and anionic CBBR-250 dye. The change in absorbance value (525 in acidic medium and 540 in basic medium) is due to ion exchange and hydrogen bonding. Conversely, at higher pH, the concentration of hydrogen ion became lower and competition of H^+ ion with the anionic dye molecules becomes negligible. Therefore, the interaction between catalyst and CBBR-250 dye decreased, leading to the minimum degradation rate [35]. In this study, the better efficiency for the decolorization of the dye in alkaline pH might be attributed to the efficient generation of hydroxyl radicals by NMCs with increasing concentration of OH^-.

3.4 Kinetics of CBBR-250

The kinetics of the reaction was calculated using pseudo-first order kinetics.

$$\ln(C/Co) = -kt \qquad (4)$$

where C and C_o are the concentration measured at different times, k is the reaction rate, and t is the reaction time during the reaction. The reaction rate (k) for the reduction of CBBR-250 was calculated by drawing a graph between $\ln(C/C_o)$ and t. The pseudo-first-order rate kinetics with respect to dye concentration could be used to evaluate the catalytic rate. As expected, a good linear correlation between $\ln(C_t/C_0)$ and reaction time t, was obtained (Fig. 10) [29]. The figure shows that the catalytic reduction follows perfectly the pseudo-first-order kinetics, and this was indicated by the linear regression value, $R^2 = 0.991$ for CBBR-250. The slope of the obtained straight line was considered as the K_{app} value of the reduction reaction. Accordingly, the apparent rate constants of catalytic reduction were determined as 0.042 s^{-1}.

The reduction mechanism of CBBR-250 dye was suggested. In order that electron transfer can occur from BH^{-4} donor to the acceptor dye through adsorption of the reactant molecules onto the catalyst surface and then, BH^{-4} ions are adsorbed on the surface of the AgNPs. After electron transfer to the AgNPs, the H atom forms from the hydride, next step spontaneously, electron transfer induces hydrogenation of dye, and, finally, the reduced product can be detached [17].
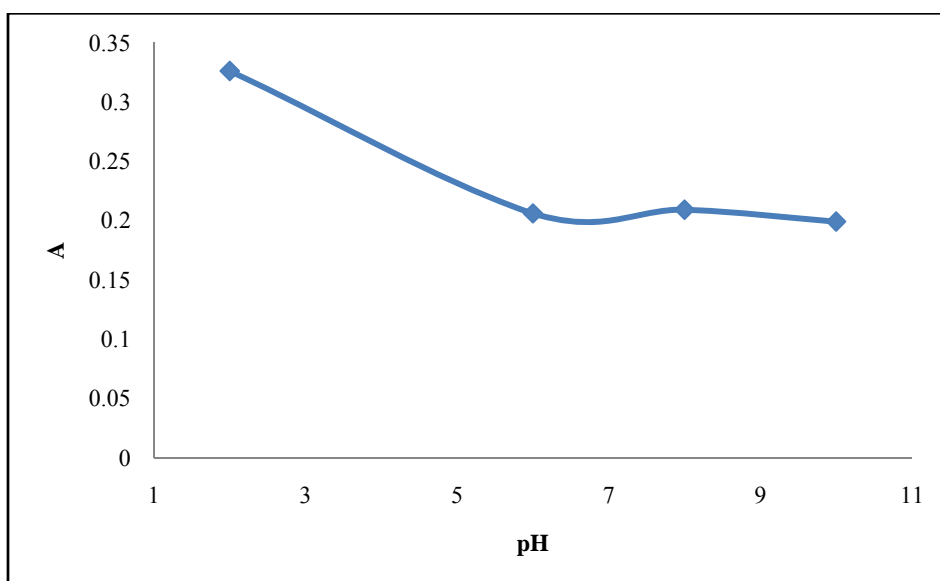
Fig. 9   UV-Visible spectra for catalytic reduction of CBBR-250 in the presence of 50 mg MNCs, 10 mM NaBH$_4$ and 0.04 mM CBBR-250 dye at different pH values.

Table 1   Comparative studies of different nanomaterials.

Sr. No.	Catalyst	Amount of catalyst in 100 mL	Agent	Dye conc.	pH	Time	Reference
1	Starch/poly(alginic acid-cl-acrylamide)nanohydrogel) ST/PL(AA-cl-AAm)NHG	0.44 mg	Alginic acid, Acrylamine = 0.1 M	20 mgL^{-1}	5	150 min	[35]
2	Dextran aldehyde-modified horseradish peroxidase	3,300 mg	H$_2$O$_2$ = 9.6 mg/L	6.4 mg/L	5	5 min	[36]
3	Iron NPs	520 mg	3% H$_2$O$_2$	250 mg/L	5	60 min	[37]
4	Fe^{2+}		H$_2$O$_2$ = (1 × 10^{-4})	(31 × 10^{-5})	3	30 min	[38]
5	Fe$_3$O$_4$ magnetism nanoparticles	7 mg	100 µmol/L H$_2$O$_2$	0.15 g/L	0.65	20 min	[39]
6	CuNPs (greens synthesized)	10 mg	Cuso$_4$.5H$_2$O	10 mg/L	5	30 min	[40]
7	BMTF functionalized ZnO nanoparticles	20 mg	Zn acetate hydrates dihydrate	0.04 mM	3	120 min	[41]
8	Ag@Fe$_3$O$_4$	16.5 mg	10 mM NaBH$_4$	0.04 mM	8	20 min	Present work

Proposed Reduction Process

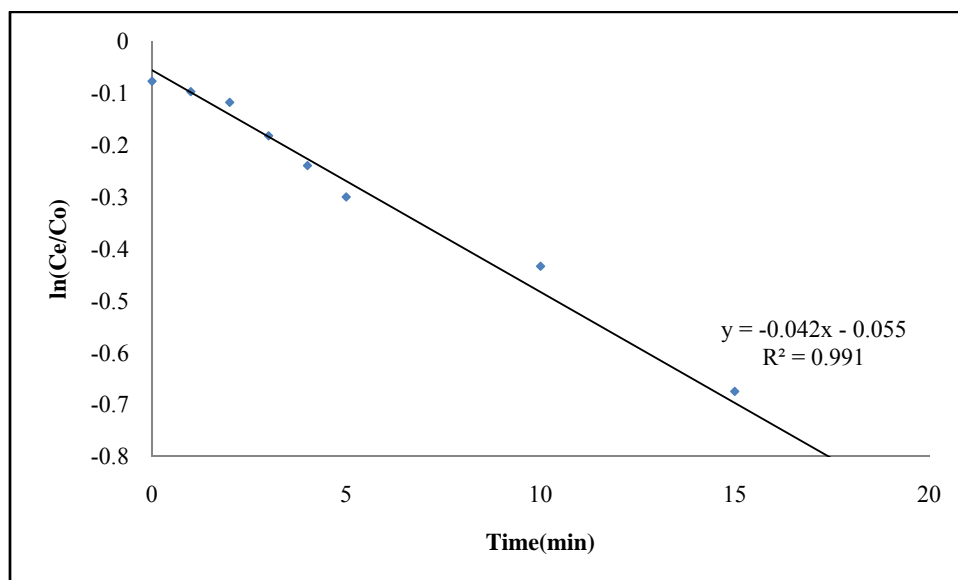$$2BH_4^- + H_2O \longrightarrow BO_2^- + 4H_2$$
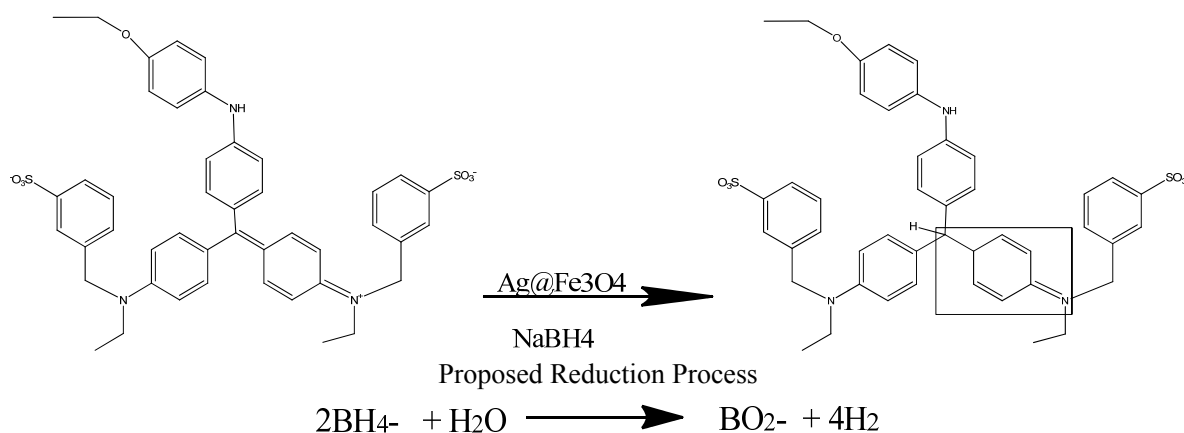
Fig. 10   Plot of ln(C_e/C_0) verses time for the reduction of CBBR-250.

Moreover, TLC (thin layer chromatography) is also performed and it is proved that reduced product R_f value is same as that of dye (original) molecule.

The FTIR spectral analysis exposed the various functional groups which are detected on the original dye (solid form) and degraded dye (after treated by MNCs). Some peaks were shifted, disappeared and new peaks were also detected in the RBBR dye (treated by MNCs) four significant bands at 3,444, 2,360 and 1,570 which indicated the bonds, -OH groups, N-H stretching and -C-C- were increased.

4. Conclusion

In this study, the AgNPs and magnetic iron oxide nanoparticles were prepared by very easy, reliable and robust method. AgNPs were adsorbed on the magnetic particles so that they were easily separated from the solution using a magnet. These MNCs were characterized by UV-visible and FTIR. Physical properties such as bulk density, moisture content and ash content were also determined. Catalytic reduction of 4-NP and reduction of CBBR-250 were studied by using these MNCs. The experimental results revealed the use of these MNCs as a reliable method for the catalytic reduction of 4-NP and reduction of CBBR-250. The kinetic analysis shows that the catalytic reduction follows perfectly the pseudo-first-order, and this is indicated by the linear regression value, $R^2 = 0.922$ and 0.931 for CBBR-250 and 4-NP, respectively. It was also found that these MNCs have efficient catalytic activity.

The major advantage of these NMCs is that separation is easy so they are recyclable. NMCs are less hazardous to environment.

Reference

[1]   Tran, Q. H., and Le, A.-T. 2013. "Silver Nanoparticles: Synthesis, Properties, Toxicology, Applications and Perspectives." *Advances in Natural Sciences: Nanoscience and Nanotechnology* 4 (3): 033001.

[2]   Dong, F., Valsami-Jones, E., and Kreft, J.-U. 2016. "New, Rapid Method to Measure Dissolved Silver Concentration in Silver Nanoparticle Suspensions by Aggregation Combined with Centrifugation." *Journal of Nanoparticle Research* 18 (9): 259.

[3]   Wu, M., et al. 2017. *Removal of Silver Nanoparticles by Mussel-Inspired Fe₃O₄@ Polydopamine Core-Shell Microspheres and Its Use as Efficient Catalyst for Methylene Blue Reduction*. Scientific Reports, p. 42773.

[4]   Alzahrani, E., 2015. "Photodegradation of Eosin Y Using Silver-Doped Magnetic Nanoparticles." *International Journal of Analytical Chemistry*, 11.

[5]   Mwilu, S. K., et al. 2014. "Separation and Measurement of Silver Nanoparticles and Silver Ions Using Magnetic Particles." *Science of the Total Environment* 472: 316-23.

[6]   Unni, M., et al. 2017. "Thermal Decomposition Synthesis

of Iron Oxide Nanoparticles with Diminished Magnetic Dead Layer by Controlled Addition of Oxygen." *ACS Nano* 11 (2): 2284-303.

[7] Bhavani, P., et al. 2017. "Synthesis of High Saturation Magnetic Iron Oxide Nanomaterials via Low Temperature Hydrothermal Method." *Journal of Magnetism and Magnetic Materials* 426: 459-66.

[8] Ansari, M. O., et al. 2017. "Iron Oxide Nanoparticles-Synthesis, Surface Modification, Applications and Toxicity: A Review." *Materials Focus* 6 (3): 269-79.

[9] Xu, P., et al. 2012. "Use of Iron Oxide Nanomaterials in Wastewater Treatment: A Review." *Science of the Total Environment* 424: 1-10.

[10] Bano, M., et al. 2016. "Hierarchical Synthesis of Silver Monoliths and Their Efficient Catalytic Activity for the Reduction of 4-Nitrophenol to 4-Aminophenol." *New Journal of Chemistry* 40 (8): 6787-95.

[11] Salmi, T., et al. 2013. "Microreactors as Tools in Kinetic Investigations: Ethylene Oxide Formation on Silver Catalyst." *Chemical Engineering Science* 87: 306-14.

[12] Ganaie, S., et al. 2014. "Biomimetic Synthesis of Silver Nanoparticles Using the Amphibious Weed Ipomoea and Their Application in Pollution Control." *Journal of King Saud University-Science* 26 (3): 222-9.

[13] Bhakya, S., et al. 2015. "Catalytic Degradation of Organic Dyes Using Synthesized Silver Nanoparticles: A Green Approach." *J Bioremed Biodeg* 6 (312): 2.

[14] Bhankhar, A., et al. 2014. "Study on Degradation of Methyl Orange-an Azo Dye by Silver Nanoparticles Using UV-Visible Spectroscopy." *Indian Journal of Physics* 88 (11): 1191.

[15] Varadavenkatesan, T., Selvaraj, R., and Vinayagam, R. 2019. "Dye Degradation and Antibacterial Activity of Green Synthesized Silver Nanoparticles Using *Ipomoea digitata* Linn. Flower Extract." *International Journal of Environmental Science and Technology* 16 (5): 2395-404.

[16] Xie, Y., et al. 2014. "Highly Regenerable Mussel-Inspired Fe$_3$O$_4$@ Polydopamine-Ag Core-Shell Microspheres as Catalyst and Adsorbent for Methylene Blue Removal." *ACS Applied Materials & Interfaces* 6 (11): 8845-52.

[17] Veisi, H., et al. 2019. "Silver Nanoparticles Decorated on Thiol-Modified Magnetite Nanoparticles (Fe$_3$O$_4$/SiO$_2$-Pr-S-Ag) as a Recyclable Nanocatalyst for Degradation of Organic Dyes." *Materials Science and Engineering: C* 97: 624-31.

[18] Sathishkumar, P., Arulkumar, M., and Palvannan, T. 2012. "Utilization of Agro-Industrial Waste Jatropha curcas Pods as an Activated Carbon for the Adsorption of Reactive Dye Remazol Brilliant Blue R (RBBR)." *Journal of Cleaner Production* 22 (1): 67-75.

[19] Chauhan, J., Mehto, V. R., and Tiwari, T. 2019. "Chemical Synthesis and Study of Silver Nanoparticles." *International Journal of Nanomaterials and Nanostructures* 5 (1): 12-7.

[20] Mavani, K., and Shah, M. 2013. "Synthesis of Silver Nanoparticles by Using Sodium Borohydride as a Reducing Agent." *Int. J. Eng. Res. Technol* 2 (3).

[21] Baig, R. N., and Varma, R. S. 2012. "A Highly Active Magnetically Recoverable Nano Ferrite-Glutathione-Copper (Nano-FGT-Cu) Catalyst for Huisgen 1, 3-Dipolar Cycloadditions." *Green Chemistry* 14 (3): 625-32.

[22] Bhangale, H., et al. 2020. "Green Synthesis of Silver Nanoparticles Using Mushroocm Species, Their Characterization and Catalytic Activity." In *Techno-Societal 2018*, 329-35.

[23] MA Golsefidi, B. S. 2017. "Preparation and Characterization of Rapid Magnetic Recyclable Fe$_3$O$_4$@ SiO$_2$@TiO$_2$-Sn Photocatalyst." *Journal of the Iranian Chemical Society*.

[24] Akın Sahbaz, D., Yakar, A., and Gündüz, U. 2019. "Magnetic Fe$_3$O$_4$-Chitosan Micro-and Nanoparticles for Wastewater Treatment." *Particulate Science and Technology* 37 (6): 732-40.

[25] Ma, J., Wang, K., and Zhan, M. 2015. "Growth Mechanism and Electrical and Magnetic Properties of Ag-Fe$_3$O$_4$ Core–Shell Nanowires." *ACS Applied Materials & Interfaces* 7 (29): 16027-39.

[26] Begum, R., et al. 2017. "Catalytic Reduction of 4-Nitrophenol Using Silver Nanoparticles-Engineered Poly (N-isopropylacrylamide-co-acrylamide) Hybrid Microgels." *Applied Organometallic Chemistry* 31 (2).

[27] Al-Marhaby, F., and Seoudi, R. 2016. "Preparation and Characterization of Silver Nanoparticles and Their Use in Catalytic Reduction of 4-Nitrophenol." *World Journal of Nano Science and Engineering* 6 (01): 29.

[28] Bouazizi, N., et al. 2018. "Silver Nanoparticle Embedded Copper Oxide as an Efficient Core-Shell for the Catalytic Reduction of 4-Nitrophenol and Antibacterial Activity Improvement." *Dalton Transactions* 47 (27): 9143-55.

[29] Ayad, M. M., et al. 2018. "Polypyrrole-Coated Cotton Fabric Decorated with Silver Nanoparticles for the Catalytic Removal of P-nitrophenol from Water." *Cellulose* 25 (12): 7393-407.

[30] Santhosh, A., Sandeep, S., and Swamy, N. K. 2019. "Green Synthesis of Nano Silver from *Euphorbia geniculata* Leaf Extract: Investigations on Catalytic Degradation of Methyl Orange Dye and Optical Sensing of Hg2+." *Surfaces and Interfaces* 14: 50-4.

[31] Amir, M., Kurtan, U., and Baykal, A. 2015. "Rapid Color Degradation of Organic Dyes by Fe$_3$O$_4$@ His@ Ag Recyclable Magnetic Nanocatalyst." *Journal of Industrial*

and Engineering Chemistry 27: 347-53.

[32] Saikia, P., Miah, A. T., and Das, P. P. 2017. "Highly Efficient Catalytic Reductive Degradation of Various Organic Dyes by Au/CeO$_2$-TiO$_2$ Nano-Hybrid." *Journal of Chemical Sciences* 129 (1): 81-93.

[33] Yao, T., et al. 2014. "A Simple Way to Prepare Au@ Polypyrrole/Fe$_3$O$_4$ Hollow Capsules with High Stability and Their Application in Catalytic Reduction of Methylene Blue Dye." *Nanoscale* 6 (13): 7666-74.

[34] Crini, G., and Badot, P.-M. 2008. "Application of Chitosan, a Natural Aminopolysaccharide, for Dye Removal from Aqueous Solutions by Adsorption Processes Using Batch Studies: A Review of Recent Literature." *Progress in Polymer Science* 33 (4): 399-447.

[35] Sharma, G., et al. 2017. "Efficient Removal of Coomassie Brilliant Blue R-250 Dye Using Starch/Poly (Alginic acid-cl-acrylamide) Nanohydrogel." *Process Safety and Environmental Protection* 109: 301-10.

[36] Altikatoglu, M., and Celebi, M. 2011. "Enhanced Stability and Decolorization of Coomassie Brilliant Blue R-250 by Dextran Aldehyde-Modified Horseradish Peroxidase." *Artificial Cells, Blood Substitutes, and Biotechnology* 39 (3): 185-90.

[37] Truskewycz, A., Shukla, R., and Ball, A. S. 2016. "Iron Nanoparticles Synthesized Using Green Tea Extracts for the Fenton-Like Degradation of Concentrated Dye Mixtures at Elevated Temperatures." *Journal of Environmental Chemical Engineering* 4 (4): 4409-17.

[38] Rayaroth, M. P., Aravind, U. K., and Aravindakumar, C. T. 2015. "Sonochemical Degradation of Coomassie Brilliant Blue: Effect of Frequency, Power Density, pH and Various Additives." *Chemosphere* 119: 848-55.

[39] Liang, A. 2013. "Study on Fe$_3$O$_4$ Magnetism Nanoparticle Catalytic Degradation of Brilliant Blue Dye in Wastewater." *Advance Materials Research* 726-731: 2960-3.

[40] Sankar, R., et al. 2014. "Green Synthesis of Colloidal Copper Oxide Nanoparticles Using Carica Papaya and Its Application in Photocatalytic Dye Degradation." *Spectrochimica Acta Part A: Molecular and Biomolecular Spectroscopy* 121: 746-50.

[41] Chaudhary, S., et al. 2016. "1-Butyl-3-Methylimidazolium Tetrafluoroborate Functionalized ZnO Nanoparticles for Removal of Toxic Organic Dyes." *Journal of Molecular Liquids* 220: 1013-21.